

This document is confidential and is proprietary to the American Chemical Society and its authors. Do not copy or disclose without written permission. If you have received this item in error, notify the sender and delete all copies.

Impacts of biofilm properties on start-up and performance of membrane biofilm reactor performing anammox and nitrate/nitrite-dependent anaerobic methane oxidation integrated processes: A model-based investigation

Journal:	<i>ACS ES&T Water</i>
Manuscript ID	ew-2022-00612q
Manuscript Type:	Article
Date Submitted by the Author:	30-Nov-2022
Complete List of Authors:	Chen, Xinyan; Fuzhou University Wang, Dongbo; College of Environmental Science and Engineering, Hunan University, Changsha 410082, China Nie, Wen-Bo; Harbin Institute of Technology, School of Environment, State Key Laboratory of Urban Water Resource and Environment Yang, Linyan; East China University of Science and Technology, Wei, Wei; University of Technology Sydney, Ni, Bing-Jie; University of Technology Sydney, School of Civil & Environmental Engineering Chen, Xueming; Fuzhou University,

SCHOLARONE™
Manuscripts

1
2
3
4 **Impacts of biofilm properties on start-up and performance of membrane biofilm**
5
6 **reactor performing anammox and nitrate/nitrite-dependent anaerobic methane**
7
8 **oxidation integrated processes: A model-based investigation**
9
10
11
12
13

14 Xinyan Chen¹, Dongbo Wang², Wen-Bo Nie³, Linyan Yang⁴, Wei Wei⁵, Bing-Jie Ni⁵,

16
17 Xueming Chen^{1*}
18
19
20
21

22 ¹Fujian Provincial Engineering Research Center of Rural Waste Recycling Technology,
23
24 College of Environment and Safety Engineering, Fuzhou University, Fuzhou 350116,
25
26
27 China
28

29
30 ²College of Environmental Science and Engineering, Hunan University, Changsha
31
32 410082, China
33

34
35 ³Key Laboratory of the Three Gorges Reservoir Region's Eco-Environment, Ministry
36
37 of education, College of Environment and Ecology, Chongqing University, Chongqing
38
39 400045, China
40
41

42
43 ⁴School of Resources and Environmental Engineering, East China University of
44
45 Science and Technology, Shanghai 200237, China
46
47

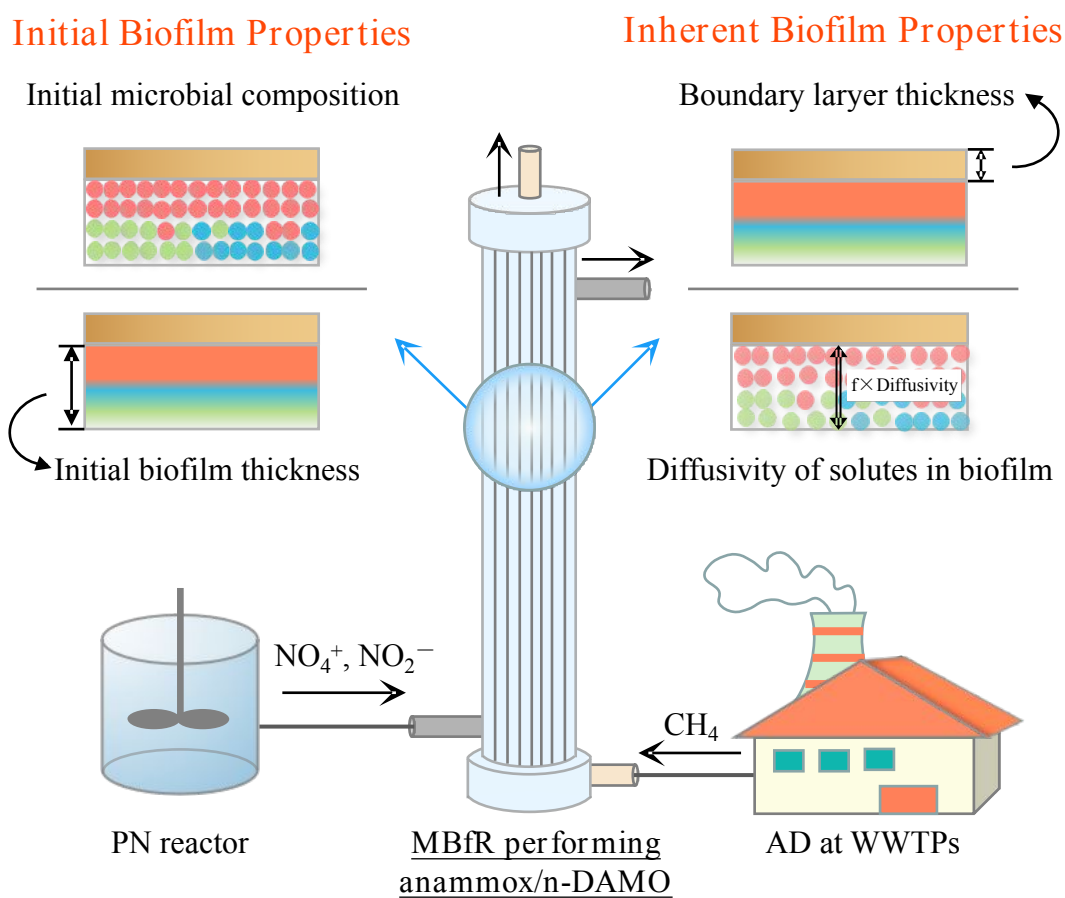
48 ⁵Centre for Technology in Water and Wastewater, School of Civil and Environmental
49
50 Engineering, University of Technology Sydney, Sydney, NSW 2007, Australia
51
52
53

54
55
56 ***Corresponding author:**
57

58 Dr. Xueming Chen, E-mail: xuem.chen@hotmail.com
59
60

Synopsis: Impacts of key biofilm properties were investigated to obtain practical guidance for the rapid establishment of the MBfR with a high-level treatment capacity based on the anammox/n-DAMO integrated processes.

GRAPHICAL ART



ABSTRACT

Even though the membrane biofilm reactor (MBfR) performing the anammox and nitrate/nitrite-dependent anaerobic methane oxidation (n-DAMO) integrated processes has been known to enable complete nitrogen removal, the effects of key biofilm properties on such a promising MBfR are yet to be disclosed. In this work, a biofilm model was constructed to investigate the effects of the initial microbial composition of the biofilm, the initial biofilm thickness, the boundary layer thickness of the biofilm, and the diffusivity of solutes in the biofilm structure on the start-up process and the steady-state performance of the MBfR performing anammox/n-DAMO. The results showed that even though the four biofilm properties studied wouldn't affect the steady-state total nitrogen removal performance, they would significantly regulate the start-up time of the MBfR. Unless the MBfR was operated under undesired operational conditions (e.g., influent $\text{NH}_4^+\text{-N}/\text{NO}_2^-\text{-N}$ ratio of 2:3 in this work), inoculation of sludge comprised mainly of anammox bacteria or/and n-DAMO archaea to form a relatively thin initial biofilm would expectedly accelerate the start-up process of the MBfR. Moreover, measures could be taken during the operation to reduce the boundary layer thickness and the diffusivity of solutes in the biofilm structure, the latter of which would also enhance the methane utilization of the MBfR. This work would provide valuable practical guidance for the rapid establishment of the MBfR with a high-level treatment capacity based on the anammox/n-DAMO integrated processes.

Keywords: anammox; biofilm properties; membrane biofilm reactor (MBfR); modeling; nitrate/nitrite-dependent anaerobic methane oxidation (n-DAMO)

1. INTRODUCTION

Anammox is a sustainable biological nitrogen removal (BNR) technology without the need for organic carbon sources and aeration^{1, 2}. Nevertheless, anammox will inevitably produce nitrate^{3, 4} and thus ought to be coupled with other microbial processes to achieve complete nitrogen removal. The discovery of nitrate/nitrite-dependent anaerobic methane oxidation (n-DAMO) processes provides a crucial BNR alternative by adopting CH₄ as the electron donor^{5, 6}. Therefore, the combination of anammox and n-DAMO processes would enable complete nitrogen removal by utilizing CH₄ produced directly on site of wastewater treatment plants^{7, 8}. Considering the low solubility of methane (i.e., 22 mg CH₄ L⁻¹ at 1 atm and 20.0 °C)⁹ and the slow growth of both anammox and n-DAMO microorganisms^{10, 11}, the membrane biofilm reactor (MBfR) configuration was proposed and applied to take on this integrated BNR technology¹²⁻²⁰. In such an MBfR, microorganisms attach onto the membrane surface and form a biofilm with methane diffusing from the membrane lumen to the biofilm and soluble substances provided (e.g., NH₄⁺ and NO₂⁻) entering the biofilm from the liquid bulk.

However, various factors could affect the performance of an MBfR and hence hinder its large-scale applications to the anammox/n-DAMO integrated processes. Therein lie the initial biofilm properties (e.g., the initial microbial composition of the biofilm and the initial biofilm thickness) and the inherent biofilm properties (e.g., the boundary layer thickness of the biofilm and the diffusivity of solutes in the biofilm structure)

1
2
3
4 which have been shown to influence the practical operation of biofilm-based reactors
5
6²¹⁻²⁴. Firstly, changes in microbial composition during the operation have been
7
8
9 demonstrated to exert a distinct influence on the performance of the MBfR¹⁷, thus
10
11 highlighting the potentially critical role of the initial microbial composition of the
12
13 biofilm. Secondly, the initial biofilm thickness has been known as a key parameter
14
15 regulating the mass transfer²⁵ and would therefore influence the substrates acquisition
16
17 by microorganisms, the evolution of the microbial structure²⁶, and the start-up process
18
19 of the MBfR. Thirdly, the boundary layer of the biofilm as an external resistance would
20
21 influence bilateral solutes exchange, which might create discrepancies in both the
22
23 removal of pollutants and the utilization of gas-phase substrates supplied to the MBfR
24
25^{27,28}. Lastly, the diffusivity of solutes in the biofilm structure would regulate the active
26
27 transport of substrates inside the biofilm and hence the growth of functional
28
29 microorganisms^{29,30}. Changes in the diffusivity of solutes in the biofilm structure might
30
31 conduce to the varied performance of the MBfR reported by Khlebnikov, et al.³¹.
32
33 However, the underlying impacts of the abovementioned biofilm properties on the
34
35 MBfR performing anammox/n-DAMO in terms of the reactor start-up and the steady-
36
37 state performance are yet to be disclosed and, without a doubt, require a significant
38
39 amount of experimental input.
40
41
42
43
44
45
46
47
48
49
50
51
52

53 In this case, the application of model-based tools seems a reliable alternative. Similar
54
55 efforts have been made to assess the feasibility of the MBfR performing anammox/n-
56
57 DAMO^{20, 32, 33} and the impacts of longitudinal heterogeneity³⁴ and operational
58
59
60

1
2
3
4 conditions ³⁵ on such an MBfR. Through applying a previously-reported bioprocess
5
6 model, this work further investigated the effects of biofilm properties (including the
7
8 initial microbial composition of the biofilm, the initial biofilm thickness, the boundary
9
10 layer thickness of the biofilm, and the diffusivity of solutes in the biofilm structure) on
11
12 the MBfR performing the anammox/n-DAMO integrated processes. In addition to the
13
14 total nitrogen (TN) removal and methane utilization efficiencies, the start-up time
15
16 needed for the MBfR to reach the steady state was also included in the judging criteria
17
18 since the typical operation of such an MBfR was featured with a long start-up process
19
20 ^{12, 13, 16, 36}. The results obtained would expectedly provide important operational
21
22 guidance for the rapid establishment of the MBfR with a high-level treatment capacity
23
24 based on the coupling of anammox with n-DAMO.
25
26
27
28
29
30
31
32
33
34

35 **2. MATERIALS AND METHODS**

36 **2.1. Bioprocess Model**

37
38 The bioprocess model developed and validated experimentally by Chen, et al. ³³ to
39
40 describe microbial interactions between anammox bacteria and n-DAMO
41
42 microorganisms was directly adopted in this work. As shown in **Tables S1** and **S2** in
43
44 the supporting information (**SI**), the model involves four functional microorganisms
45
46 (i.e., anammox bacteria (X_{An}), n-DAMO archaea (X_{Da}), n-DAMO bacteria (X_{Db}), and
47
48 heterotrophic bacteria (X_{HB})) which are collectively responsible for the conversions of
49
50 6 soluble components (including ammonium (S_{NH4}), nitrite (S_{NO2}), nitrate (S_{NO3}),
51
52 nitrogen gas (S_{N2}), methane (S_{CH4}), and readily biodegradable organics (S_S)) and 2 solid
53
54
55
56
57
58
59
60

1
2
3
4 components (i.e., slowly biodegradable biomass (X_S) and inert biomass (X_I)). Briefly,
5
6 anammox bacteria can use ammonium as the electron donor to reduce nitrite and
7
8 produce mainly nitrogen gas and some nitrate. With methane as the electron donor, n-
9
10 DAMO archaea can reduce nitrate to nitrite while n-DAMO bacteria can further convert
11
12 nitrite to nitrogen gas ^{5,6}. In addition to conventional substrate-based Monod terms, the
13
14 reported inhibition of NO_2^- on anammox bacteria and n-DAMO microorganisms are
15
16 considered in the model, the details of which (i.e., values of stoichiometric and kinetic
17
18 parameters) are summarized in **Table S3**.
19
20
21
22
23
24
25
26

27 **2.2. Reactor Configuration**

28
29 Referring to Chen, et al. ³³, the total volume of the MBfR simulated in this work was
30
31 1.0 m³, consisting of 0.04 m³ membrane lumen and 0.96 m³ biofilm reactor, while the
32
33 total biofilm area was set at 235.0 m². A diffusive mode was used to link the biofilm
34
35 reactor to the membrane lumen, which was assumed to be operated in an open-end
36
37 mode to avoid the presence of gas back-diffusion. Variations in the methane supply
38
39 were achieved by changing the methane flow rate at a constant gas pressure of 10 kPa.
40
41 The counter-diffusional provision of the liquid-phase substrates (i.e., $\text{NH}_4^+\text{-N}$ and
42
43 $\text{NO}_2^-\text{-N}$) and the gas-phase methane into the biofilm was driven by concentration
44
45 gradients as described by Fick's law. As shown in **Table S4**, the mass transfer
46
47 coefficient of methane from the membrane lumen to the biofilm and the substrate
48
49 diffusion coefficients in water were adapted from Chen, et al. ³³ and Haynes ³⁷,
50
51 respectively. The mass transfer resistance between the liquid phase and the biofilm
52
53
54
55
56
57
58
59
60

1
2
3
4 matrix was introduced by the boundary layer, while the mass transfer resistance from
5
6 the membrane lumen to the biofilm was not specifically accounted for in this work ³⁸.
7

8
9 Other operational parameters of the MBfR are listed in **Table S4**.
10

11 12 13 14 **2.3. Simulation Scenarios**

15
16 The model platform AQUASIM ³⁹ with the implementation of the bioprocess mode
17 introduced in **Section 2.1** was applied to study the effects of critical biofilm properties
18 on the MBfR configured according to **Section 2.2**. The ideal operational conditions
19 reported by Chen, et al. ³³ and Chen, et al. ³⁴ were applied to simulate the treatment of
20 sidestream wastewater with an influent TN (i.e, the sum of $\text{NH}_4^+\text{-N}$ and $\text{NO}_2^-\text{-N}$)
21 concentration of 500.0 g N m^{-3} , which included an influent ratio of $\text{NH}_4^+\text{-N}$ to $\text{NO}_2^-\text{-N}$
22 of 1:1 and a CH_4 surface loading of $0.064 \text{ g COD m}^{-2} \text{ d}^{-1}$. As shown in **Table 1**,
23 scenarios 1 to 4 were designed to explore the effects of the initial microbial composition
24 of the biofilm ($R_{\text{An:Da:Db}}$), the initial biofilm thickness (L_f), the boundary layer thickness
25 of the biofilm (LBL), and the reduction factor for diffusivity of solutes in the biofilm
26 structure (f , as compared with the diffusion coefficients of solutes in water),
27 respectively, on the start-up time and the steady-state TN removal and methane
28 utilization efficiencies of the MBfR performing anammox/n-DAMO. Scenarios 1 to 4
29 were also simulated under the operational conditions that deviated from the reported
30 ideal ones to verify the general applicability of the results. As presented in **Table 1**, the
31 influent ratio of $\text{NH}_4^+\text{-N}$ to $\text{NO}_2^-\text{-N}$ was adjusted to 2:3 and 3:2 while the CH_4 surface
32 loading was varied to 0.032 and $0.128 \text{ g COD m}^{-2} \text{ d}^{-1}$. Each simulation scenario was
33
34
35
36
37
38
39
40
41
42
43
44
45
46
47
48
49
50
51
52
53
54
55
56
57
58
59
60

run to reach the steady state, and the time needed was recorded as the start-up time. The steady-state TN removal and CH₄ utilization efficiencies calculated by **Eqs. 1** and **2**, respectively, and the microbial composition of the biofilm together with the start-up time were used to comprehensively evaluate the impacts of the biofilm properties studied on the MBfR performing anammox/n-DAMO.

Table 1. Overview of simulation scenarios.

Scenarios	Biofilm properties	Substrates conditions
<u>Scenario 1</u> Effect of initial microbial composition	R _{An:Da:Db} = (0.05-20):(0.05-20):(0.05-20) L _f = 500 μm LBL = 40 μm f = 0.5	Influent NH ₄ ⁺ -N:NO ₂ ⁻ -N = 1:1 (2:3 and 3:2) CH ₄ surface loading = 0.064 g COD m ⁻² d ⁻¹ (0.032 and 0.128 g COD m ⁻² d ⁻¹)
<u>Scenario 2</u> Effect of initial biofilm thickness	R _{An:Da:Db} = 1:1:1 L _f = 50-500 μm LBL = 40 μm f = 0.5	
<u>Scenario 3</u> Effect of boundary layer thickness	R _{An:Da:Db} = 1:1:1 L _f = 500 μm LBL = 0-120 μm f = 0.5	
<u>Scenario 4</u> Effect of reduction factor of diffusivity of solutes in biofilm structure	R _{An:Da:Db} = 1:1:1 L _f = 500 μm LBL = 40 μm f = 0.2-0.8	

The substrates conditions inside brackets were used to verify the general applicability of the results obtained under ideal operational conditions outside brackets.

$$\text{TN removal efficiency} = \left(1 - \frac{S_{\text{NH}_4,\text{eff}} + S_{\text{NO}_2,\text{eff}} + S_{\text{NO}_3,\text{eff}}}{S_{\text{NH}_4,\text{in}} + S_{\text{NO}_2,\text{in}}}\right) \times 100\% \quad (\text{Eq. 1})$$

where $S_{\text{NH}_4,\text{in}}$ and $S_{\text{NO}_2,\text{in}}$ represent the influent concentrations of NH₄⁺ and NO₂⁻ (g N m⁻³), respectively; $S_{\text{NH}_4,\text{eff}}$, $S_{\text{NO}_2,\text{eff}}$ and $S_{\text{NO}_3,\text{eff}}$ represent the effluent concentrations of

1
2
3
4 NH_4^+ , NO_2^- and NO_3^- (g N m^{-3}), respectively.
5
6
7

8
9
$$\text{CH}_4 \text{ utilization efficiency} = \left(1 - \frac{\text{CH}_{4, \text{out}}}{\text{CH}_{4, \text{loading}} - \text{CH}_{4, \text{gas}}} \right) \times 100\% \quad (\text{Eq. 2})$$

10
11 where $\text{CH}_{4, \text{loading}}$ is the CH_4 loading into the membrane lumen ($\text{g COD m}^{-2} \text{ d}^{-1}$); $\text{CH}_{4, \text{gas}}$
12 is the CH_4 loading leaving the membrane lumen ($\text{g COD m}^{-2} \text{ d}^{-1}$); $\text{CH}_{4, \text{out}}$ is the
13 dissolved CH_4 loading in the effluent ($\text{g COD m}^{-2} \text{ d}^{-1}$).
14
15
16
17
18
19
20
21

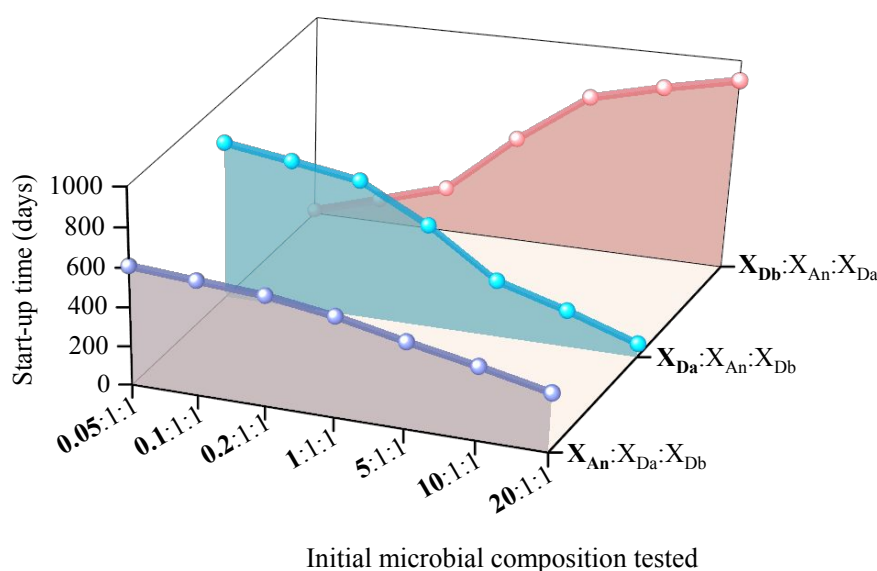
22 **3. RESULTS AND DISCUSSION**

23 **3.1. Effects of Properties of Initial Biofilm**

24 **3.1.1 Initial microbial composition of biofilm (Scenario 1)**

25
26
27
28
29
30 As shown in **Fig. 1** and **Table S5**, changes in the initial microbial composition of the
31 biofilm were found to not affect the steady-state biomass composition (mainly with
32 anammox bacteria (74.4%) and n-DAMO archaea (15.2%)), the TN removal efficiency
33 (98.8%), and the CH_4 utilization efficiency (85.2%) under the reported ideal operational
34 conditions, but exert a significant influence on the start-up time required for the MBfR
35 to achieve the steady-state operation. To be specific, with the increasing initial
36 proportion of anammox bacteria or n-DAMO archaea in the biofilm, the MBfR could
37 reach the steady state faster which was due to the dominance of anammox bacteria and
38 n-DAMO archaea at the steady state and their close cooperation for complete nitrogen
39 removal. Comparatively, the initial proportion of n-DAMO archaea was found to play
40 a more profound role in regulating the start-up process of the MBfR: the start-up time
41 was significantly shortened from 789 to 67 days when the initial $X_{\text{Da}}:X_{\text{An}}:X_{\text{Db}}$ ratio was
42
43
44
45
46
47
48
49
50
51
52
53
54
55
56
57
58
59
60

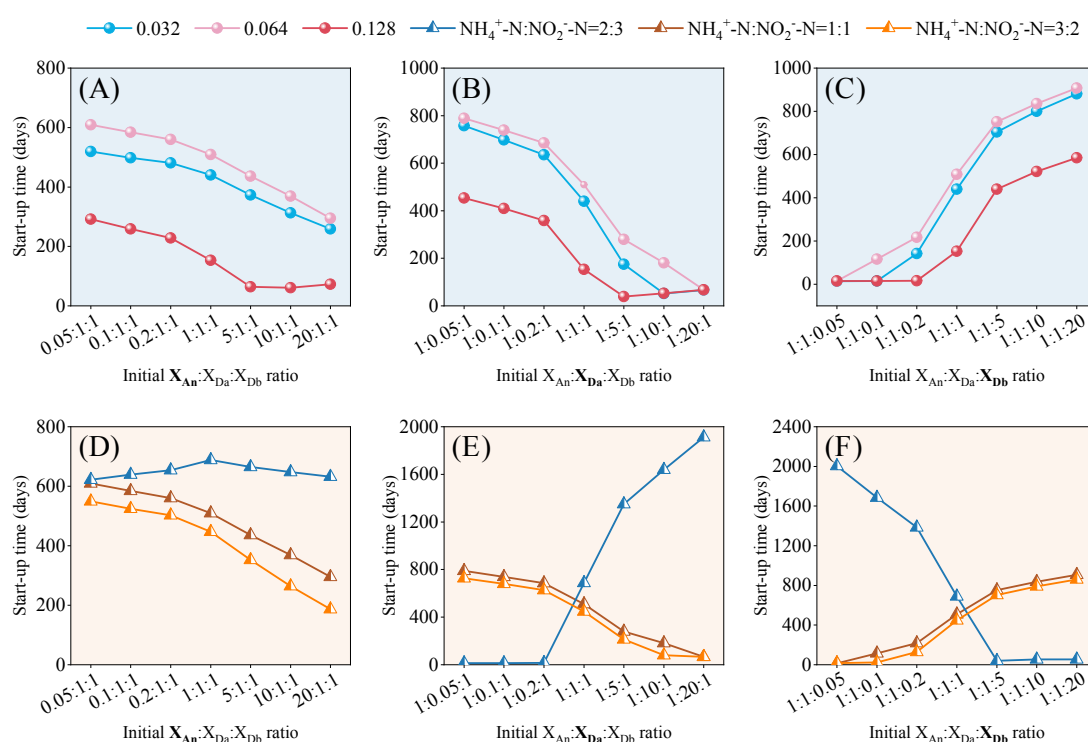
1
2
3
4 elevated from 0.05:1:1 to 20:1:1. This phenomenon resulted from the essentially
5
6 inferior and slow growth of n-DAMO archaea which depended on the functioning of
7
8 anammox bacteria to produce nitrate. Analogously, the increase in the initial proportion
9
10 of n-DAMO bacteria in the biofilm prolonged the start-up time since it hindered the
11
12 growth of anammox bacteria and n-DAMO archaea through substrate competition and
13
14 therefore requested more time to wash n-DAMO bacteria out of the biofilm.
15
16
17
18
19
20
21
22



23
24
25
26
27
28
29
30
31
32
33
34
35
36
37
38
39
40
41
42 **Figure 1.** Effect of the initial microbial composition ($X_{An}:X_{Da}:X_{Db}$) of the biofilm on
43
44 the time needed for the MBfR to reach the steady state at influent $NH_4^+-N/NO_2^- -N$ ratio
45
46 of 1:1 and CH_4 surface loading of $0.064 \text{ g COD m}^{-2} \text{ d}^{-1}$.
47
48
49
50
51

52 To verify the general applicability of the above findings, the simulations were repeated
53
54 under different substrates conditions, i.e., influent $NH_4^+-N/NO_2^- -N$ ratios of 2:3 and
55
56 3:2 and CH_4 surface loadings of 0.032 and $0.128 \text{ g COD m}^{-2} \text{ d}^{-1}$, as shown in **Table 1**.
57
58
59
60 Despite the overall distinct TN removal and CH_4 utilization efficiencies obtained under

different operational conditions, the initial microbial composition of the biofilm did not affect the steady-state TN removal and methane utilization efficiencies (see **Table S5**) but posed a significant impact on the start-up time, as presented in **Fig. 2**. It could be observed that when the methane loading was halved ($0.032 \text{ g COD m}^{-2} \text{ d}^{-1}$) or doubled ($0.128 \text{ g COD m}^{-2} \text{ d}^{-1}$), increasing the initial proportion of anammox bacteria or n-DAMO archaea would generally facilitate the start-up process of the MBfR, while an opposite trend was observed for the initial proportion of n-DAMO bacteria in the biofilm (**Fig. 2A-C**). As shown in **Fig. 2D-F**, an inconsistent relationship was observed at the influent $\text{NH}_4^+\text{-N}/\text{NO}_2^-\text{-N}$ ratio of 2:3. This phenomenon was due to the completely different microbial composition (i.e., the coexistence of anammox bacteria and n-DAMO bacteria without n-DAMO archaea) for ultimately incomplete nitrogen removal in the MBfR at the steady state (see **Table S5**).



1
2
3
4 **Figure 2.** Effect of the initial microbial composition of the biofilm on the time needed
5
6 for the MBfR to reach the steady state at CH₄ surface loadings of (A) 0.032, (B) 0.064
7
8 and (C) 0.128 g COD m⁻² d⁻¹, and influent NH₄⁺-N/NO₂⁻-N ratios of (D) 2:3, (E) 1:1
9
10 and (F) 3:2.
11
12
13

14 15 16 17 **3.1.2. Initial biofilm thickness (Scenario 2)**

18
19 Similarly, when the MBfR was operated under the reported ideal conditions, changes
20
21 in the initial biofilm thickness did not affect the steady-state biomass composition, with
22
23 anammox bacteria and n-DAMO archaea each accounting for 74.4% and 15.2% of the
24
25 total biomass, respectively, thus leading to the fixed TN removal efficiency of 98.8%
26
27 and CH₄ utilization efficiency of 85.2% in **Fig. 3A**. However, with the increase in the
28
29 initial biofilm thickness from 50.0 to 500.0 μm, the start-up time needed for the MBfR
30
31 to reach the stable coupling of anammox with n-DAMO was prolonged from 371 to
32
33 509 days (see **Fig. 3A**). Such an observation resulted from the intensified microbial
34
35 competition for both the limited supply of substrates (i.e., NH₄⁺-N, NO₂⁻-N and CH₄)
36
37 and the compressed growth space brought about by the elevated initial biofilm thickness,
38
39 thus extending the time needed for the biofilm to develop towards the steady state.
40
41
42
43
44
45
46
47
48
49
50
51
52
53
54
55
56
57
58
59
60

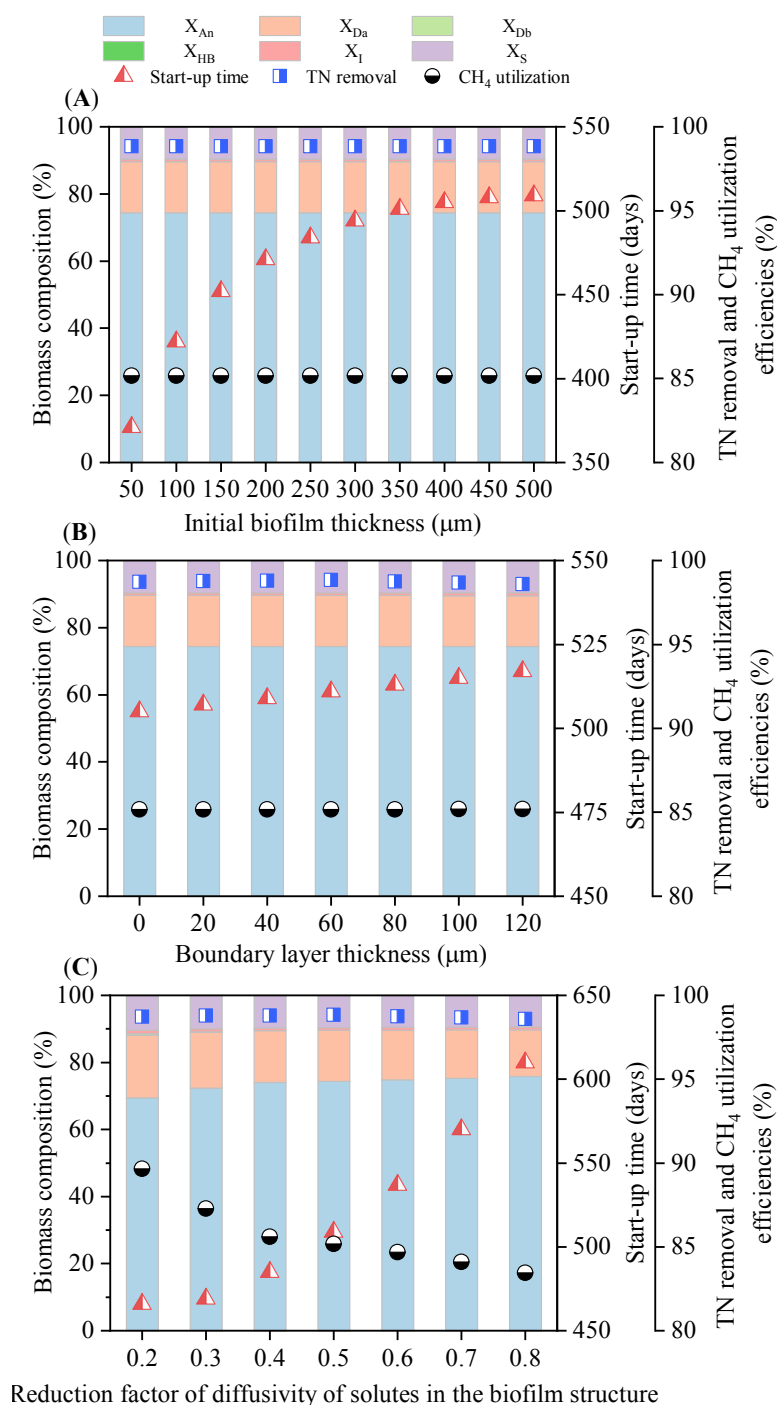


Figure 3. Effects of (A) the initial biofilm thickness, (B) boundary layer thickness and (C) reduction factor of diffusivity of solutes in the biofilm structure on the steady-state microbial composition, TN removal efficiency and CH₄ utilization efficiency, and the time needed for the MBfR to reach the steady state at influent NH₄⁺-N/NO₂⁻-N ratio of 1:1 and CH₄ surface loading of 0.064 g COD m⁻² d⁻¹.

To further test the impact of the initial biofilm thickness on the MBfR, different influent $\text{NH}_4^+\text{-N}/\text{NO}_2^-\text{-N}$ ratios of 2:3 and 3:2 and CH_4 surface loadings of 0.032 and 0.0128 $\text{g COD m}^{-2} \text{d}^{-1}$ were simulated. Regardless of the distinct results obtained under different operational conditions, similar trends that the steady-state microbial composition, TN removal efficiency, and CH_4 utilization efficiency were not sensitive to changes in the initial biofilm thickness were obtained. While the positive relationship between the start-up time and the initial biofilm thickness was also noted at the influent $\text{NH}_4^+\text{-N}/\text{NO}_2^-\text{-N}$ ratios of 2:3 and 3:2 (see **Fig. 4A**), a different trend was observed at the excessive CH_4 surface loading of 0.128 $\text{g COD m}^{-2} \text{d}^{-1}$ (see **Fig. 4B**), which led to the undesired coexistence of n-DAMO archaea and bacteria in the biofilm at the steady state (see **Table S6**).

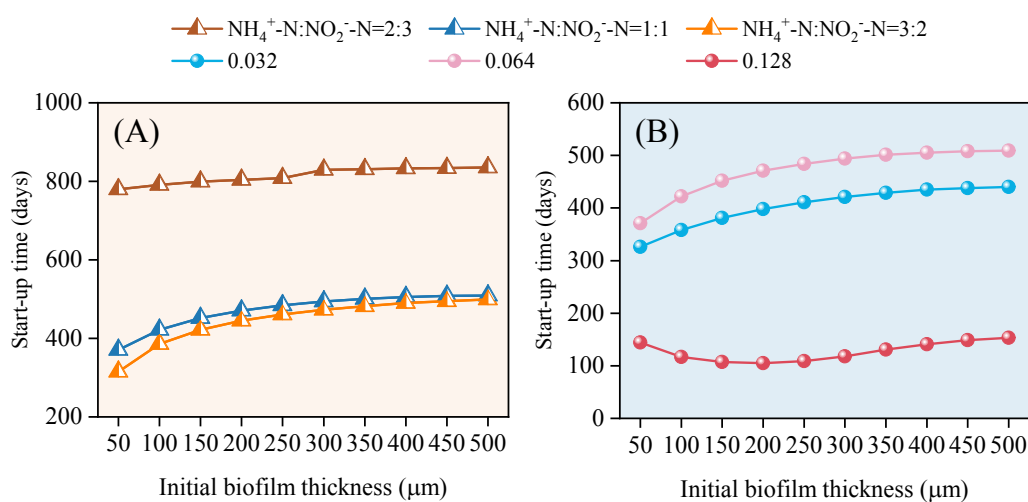


Figure 4. Effect of the initial biofilm thickness on the start-up time of the MBfR at (A) influent $\text{NH}_4^+\text{-N}/\text{NO}_2^-\text{-N}$ ratios of 2:3, 1:1 and 3:2, and (B) methane surface loadings of 0.032, 0.064 and 0.128 $\text{g COD m}^{-2} \text{d}^{-1}$.

3.2. Effects of Inherent Biofilm Properties

3.2.1 Boundary layer thickness (Scenario 3)

Based on the simulation results obtained under the reported ideal operational conditions, the boundary layer thickness was found to have no obvious effect on the biomass composition of the steady-state MBfR (**Fig. 3B**) with functional microorganisms being anammox bacteria (74.4%) and n-DAMO archaea (15.2%). In addition to the nearly unchanged TN removal efficiency of >98.0%, the resultant methane utilization efficiency stabilized at about 85.1%, which was different from the positive contribution of a boundary layer to gas utilization proposed by Martin and Nerenberg³⁸ and Nerenberg⁴⁰. The same steady-state biomass composition contributing to the consumption of methane inside the biofilm minimized the role of the boundary layer in resisting the loss of methane to the bulk liquid. Comparatively, the time needed for the MBfR to reach the steady state slightly increased from 505 to 517 days with the boundary layer thickening from 0 to 120 μm . This might be due to the elevated resistance of soluble substrates diffusing from the bulk liquid to the biofilm²⁸, thus delaying the start-up process of the MBfR. Consistent results could be observed at varied substrate conditions that were tested in this work (see **Fig. S1**).

3.2.2 Diffusivity of solutes in biofilm structure (Scenario 4)

As exhibited in **Fig. 3C**, under the reported ideal operational conditions, changes in the diffusivity of solutes in the biofilm structure had no apparent effect on the TN removal

1
2
3
4 efficiency which stayed around 98.8% but played a noticeable role in the steady-state
5
6 microbial composition and CH₄ utilization efficiency and the start-up time. With the
7
8 rising diffusivity of solutes in the biofilm structure by increasing the reduction factor
9
10 of diffusion coefficients from 0.2 to 0.8, the proportion of anammox bacteria increased
11
12 gradually from 69.5% to 75.8% (**Fig. 3C**), due to the elevated fluxes of NH₄⁺ and NO₂⁻
13
14 as the substrates for anammox bacteria from the bulk liquid into the biofilm. Meanwhile,
15
16 the increase in diffusion coefficients accelerated the passing of methane and enhance
17
18 its penetration through the biofilm, thereby reducing the methane utilization efficiency
19
20 from 89.6% to 83.4% (**Fig. 3C**) and the associated proportion of n-DAMO archaea. In
21
22 terms of the start-up time, a significant change from 466 to 610 days was observed with
23
24 the increase in diffusion coefficients of solutes in the biofilm structure. This
25
26 phenomenon was potentially attributed to the shortened effective time of contact
27
28 between microorganisms and substrates caused by rapid diffusion, hence extending the
29
30 time needed for microorganisms to grow towards the state steady.
31
32
33
34
35
36
37
38
39
40
41
42

43 The same operation under different substrate conditions rendered comparable results
44
45 (see **Fig. 5** and **Fig. S2**). Although the steady-state microbial composition differed, the
46
47 changing trend was the same: with the rise in the reduction factor of diffusivity in the
48
49 biofilm structure, the proportion of anammox bacteria increased while those of n-
50
51 DAMO microorganisms decreased (see **Fig. S2**). As exhibited in **Fig. 5**, the overall
52
53 trends of the TN removal efficiency, CH₄ utilization efficiency, and start-up time were
54
55 similar to those obtained under ideal conditions: in addition to the nearly flat TN
56
57
58
59
60

removal efficiency, the methane utilization efficiency dropped while the start-up time extended with the increasing reduction factor of diffusivity in the biofilm structure.

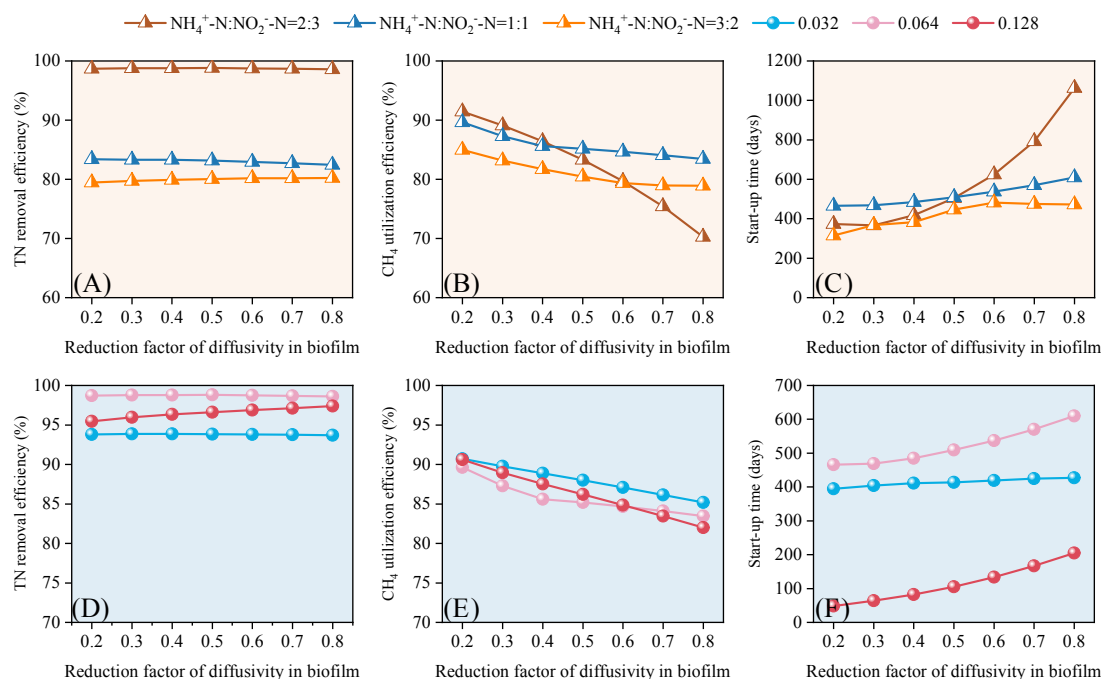


Figure 5. Effect of the reduction factor of diffusivity in the biofilm structure on the steady-state TN removal efficiency and CH₄ utilization efficiency, and the start-up time of the MBfR at influent ratios of NH₄⁺-N to NO₂⁻-N of (A) 2:3, (B) 1:1 and (C) 3:2, and CH₄ surface loadings of (D) 0.032, (E) 0.064 and (F) 0.128 g COD m⁻² d⁻¹.

3.3. Practical Implications of This Work

Although both experimental and modeling studies of the MBfR performing the anammox/n-DMO integrated processes have been reported^{8, 20, 32, 34, 35}, this work for the first time comprehensively explored the effects of key biofilm properties of on the start-up process and steady-state performance of such an MBfR. Through testing various operational conditions, the general applicability of the observations was

1
2
3
4 verified. The findings of this work would provide important guidance for improving
5
6 the operation of the MBfR, although its validity might be improved by further
7
8 experimentation.
9

10
11
12
13
14 The aforementioned simulations demonstrated that the properties of the biofilm to
15
16 initiate the MBfR including the initial microbial composition and the initial biofilm
17
18 thickness generally would not affect the steady-state microbial composition, TN
19
20 removal, and CH₄ utilization of the MBfR performing the anammox/n-DAMO
21
22 integrated processes. However, it has been observed from practical operations that
23
24 MBfRs performing anammox/n-DAMO experienced different start-up times ^{16, 36, 41},
25
26 where the contents of anammox bacteria and n-DAMO archaea in the inoculated sludge
27
28 to form the initial biofilm would be an influencing factor. This work further
29
30 demonstrated this point by clearly revealing the possibility of significantly accelerating
31
32 the start-up process of the MBfR performing the anammox/n-DAMO integrated
33
34 processes upon the availability of an initial biofilm comprised mainly of anammox
35
36 bacteria or/and n-DAMO archaea, with the latter presenting a more profound advantage.
37
38 Another important finding of this work when simulating the effects of initial biofilm
39
40 properties was that more inoculated sludge (i.e., higher initial biofilm thickness) wasn't
41
42 necessarily better for starting the MBfR. The mass transfer of substrates would drop
43
44 with the increasing biofilm thickness ^{42, 43} and thus slow down the valid growth of
45
46 microorganisms ⁴⁴. Therefore, selecting a relatively thin initial biofilm might be
47
48 conducive to high substrate transport rates ⁴³ and hence shorten the start-up time of the
49
50
51
52
53
54
55
56
57
58
59
60

1
2
3
4 MBfR performing anammox/n-DAMO.
5
6
7
8

9 The inherent properties of the biofilm including the boundary layer thickness and the
10 diffusivity of solutes in the biofilm structure were noted to play minor roles in the
11 steady-state results, which were consistent with a previous study on an autotrophic
12 deammonification-based MBfR supplied with air ²⁹. Compared with the boundary
13 layer thickness, the diffusivity of solutes in the biofilm structure was found to exert a
14 more profound impact on the start-up time of the MBfR. Therefore, keeping a thin
15 boundary thickness and low diffusivity of solutes in the biofilm structure would be
16 conducive to achieving complete TN removal and high-level CH₄ utilization whilst
17 shortening the start-up time process (see **Fig. 3B-C**). Previous studies proposed that
18 internal circulation of the liquid phase at a proper flow rate could be set to weaken the
19 boundary layer whilst compacting the biofilm structure ^{45, 46}. It needs to be mentioned
20 that the diffusivity of solutes was assumed to be homogeneous inside the biofilm in this
21 work, while it might change with the thickness/depth in practice ⁴⁷. Therefore, it
22 warrants continuous research to explore the influence of heterogeneous diffusivity of
23 solutes in the biofilm structure on the MBfR performing anammox/n-DAMO.
24
25
26
27
28
29
30
31
32
33
34
35
36
37
38
39
40
41
42
43
44
45
46
47
48
49

50 Noticeably, the abovementioned general findings regarding the critical role of proper
51 selection of inoculated sludge as the initial biofilm in the start-up process of the MBfR
52 performing anammox/n-DAMO might not be necessarily suitable for the MBfR
53 operated under undesired operational conditions of i) undue upstream partial nitrification
54
55
56
57
58
59
60

1
2
3
4 process (e.g., producing influent $\text{NH}_4^+\text{-N}/\text{NO}_2^-\text{-N}$ ratio of 2:3 studied in this work) and
5
6 ii) excessive methane supply (e.g., CH_4 surface loading of $0.128 \text{ g COD m}^{-2} \text{ d}^{-1}$ studied
7
8 in this work). These operational conditions would promote the growth of n-DAMO
9
10 bacteria as a major contributor to nitrogen transformation. Consistent with Chen, et al.
11
12 ³⁴, the such non-ideal microbial composition would not be in favor of realizing complete
13
14 nitrogen removal in the MBfR performing anammox/n-DAMO processes.
15
16
17
18
19
20
21

22 **4. CONCLUSIONS**

23
24 A one-dimensional counter-diffusional multi-species and multi-substrates biofilm
25
26 model was constructed to simulate the impacts of key biofilm properties on the MBfR
27
28 performing anammox/n-DAMO. This work showed that even though the four biofilm
29
30 properties studied wouldn't affect the steady-state total nitrogen removal performance,
31
32 they would significantly regulate the start-up time of the MBfR. Unless the MBfR was
33
34 operated under undesired operational conditions (e.g., influent $\text{NH}_4^+\text{-N}/\text{NO}_2^-\text{-N}$ ratio
35
36 of 2:3 in this work), inoculation of sludge comprised mainly of anammox bacteria
37
38 or/and n-DAMO archaea to form a relatively thin initial biofilm would expectedly
39
40 accelerate the start-up process of the MBfR. Moreover, sufficient internal circulation in
41
42 the liquid phase could be set during the operation to reduce the boundary layer thickness
43
44 and the diffusivity of solutes in the biofilm structure, the latter of which would also
45
46 enhance the methane utilization of the MBfR. This work would provide practical
47
48 guidance for the rapid establishment of the MBfR with a high-level treatment capacity
49
50 based on the anammox/n-DAMO integrated processes.
51
52
53
54
55
56
57
58
59
60

ACKNOWLEDGEMENTS

This work was supported by National Natural Science Foundation of China (grant number: 52100028) and Fuzhou University (grant number: GXRC-20095). B.-J. Ni acknowledges the Australian Research Council (ARC) through Discovery Project DP220101142. The authors declare that they have no known competing financial interests.

REFERENCES

- (1) Yang, S.; et al. Autotrophic nitrogen removal in an integrated fixed-biofilm activated sludge (IFAS) reactor: Anammox bacteria enriched in the flocs have been overlooked. *Bioresour Technol* **2019**, *288*, 121512.
- (2) Xue, Z.; et al. Integrated moving bed biofilm reactor with partial denitrification-anammox for promoted nitrogen removal: Layered biofilm structure formation and symbiotic functional microbes. *Sci Total Environ* **2022**, *839*, 156339.
- (3) Peng, L.; et al. Modeling nitrate/nitrite dependent anaerobic methane oxidation and Anammox process in a membrane granular sludge reactor. *Chem. Eng. J* **2021**, *403*, 125822.
- (4) Lackner, S.; et al. Full-scale partial nitrification/anammox experiences--an application survey. *Water Res* **2014**, *55*, 292-303.
- (5) Haroon, M. F.; et al. Anaerobic oxidation of methane coupled to nitrate reduction in a novel archaeal lineage. *Nature* **2013**, *500* (7464), 567-570.

- 1
2
3
4 (6) Raghoebarsing, A. A.; et al. A microbial consortium couples anaerobic methane
5
6 oxidation to denitrification. *Nature* **2006**, *440* (7086), 918-921.
7
8
9 (7) Liu, T.; et al. Simultaneous Removal of Dissolved Methane and Nitrogen from
10
11 Synthetic Mainstream Anaerobic Effluent. *Environ Sci Technol* **2020**, *54* (12),
12
13 7629-7638.
14
15
16 (8) Lim, Z. K.; et al. Versatility of nitrite/nitrate-dependent anaerobic methane
17
18 oxidation (n-DAMO): First demonstration with real wastewater. *Water Res* **2021**,
19
20 *194*, 116912.
21
22
23 (9) Yamamoto, S.; et al. Solubility of methane in distilled water and seawater. *Journal*
24
25 *of Chemical and Engineering Data* **1976**, *21* (1), 78-80.
26
27
28 (10) Lotti, T.; et al. Anammox growth on pretreated municipal wastewater. *Environ Sci*
29
30 *Technol* **2014**, *48* (14), 7874-7880.
31
32
33 (11) Allegue, T.; et al. Enrichment of nitrite-dependent anaerobic methane oxidizing
34
35 bacteria in a membrane bioreactor. *Chem. Eng. J* **2018**, *347*, 721-730.
36
37
38 (12) Shi, Y.; et al. Nitrogen removal from wastewater by coupling anammox and
39
40 methane-dependent denitrification in a membrane biofilm reactor. *Environ Sci*
41
42 *Technol* **2013**, *47* (20), 11577-11583.
43
44
45 (13) Cai, C.; et al. Nitrate reduction by denitrifying anaerobic methane oxidizing
46
47 microorganisms can reach a practically useful rate. *Water Res* **2015**, *87*, 211-217.
48
49
50 (14) Ding, Z. W.; et al. Simultaneous enrichment of denitrifying anaerobic methane-
51
52 oxidizing microorganisms and anammox bacteria in a hollow-fiber membrane
53
54 biofilm reactor. *Appl Microbiol Biotechnol* **2017**, *101* (1), 437-446.
55
56
57
58
59
60

- 1
2
3
4 (15) Liu, T.; et al. Temperature-Tolerated Mainstream Nitrogen Removal by Anammox
5 and Nitrite/Nitrate-Dependent Anaerobic Methane Oxidation in a Membrane
6 Biofilm Reactor. *Environ Sci Technol* **2020**, *54* (5), 3012-3021.
7
8
9
10
11 (16) Nie, W. B.; et al. Operation strategies of n-DAMO and Anammox process based
12 on microbial interactions for high rate nitrogen removal from landfill leachate.
13
14
15
16
17 *Environ Int* **2020**, *139*, 105596.
18
19 (17) Fu, L.; et al. Hollow fiber membrane bioreactor affects microbial community and
20 morphology of the DAMO and Anammox co-culture system. *Bioresour Technol*
21
22
23
24
25 **2017**, *232*, 247-253.
26
27 (18) Liu, T.; et al. Enhancing mainstream nitrogen removal by employing nitrate/nitrite-
28 dependent anaerobic methane oxidation processes. *Critical Reviews in*
29
30
31
32
33 *Biotechnology* **2019**, *39* (5), 732-745.
34
35 (19) van Kessel, M. A.; et al. Current perspectives on the application of N-damo and
36 anammox in wastewater treatment. *Curr Opin Biotechnol* **2018**, *50*, 222-227.
37
38
39 (20) Chen, X.; et al. Modeling of simultaneous anaerobic methane and ammonium
40 oxidation in a membrane biofilm reactor. *Environ Sci Technol* **2014**, *48* (16), 9540-
41
42
43
44
45
46
47 9547.
48 (21) Lackner, S.; et al. Nitrification performance in membrane-aerated biofilm reactors
49 differs from conventional biofilm systems. *Water Res* **2010**, *44* (20), 6073-6084.
50
51
52 (22) Wang, J.; et al. In-situ monitoring AHL-mediated quorum-sensing regulation of
53 the initial phase of wastewater biofilm formation. *Environ Int* **2020**, *135*, 105326.
54
55
56
57 (23) van den Berg, L.; et al. How to measure diffusion coefficients in biofilms: A critical
58
59
60

- 1
2
3
4 analysis. *Biotechnol Bioeng* **2021**, *118* (3), 1273-1285.
5
6
7 (24) Zhang, C.; et al. Locomotion of bacteria in liquid flow and the boundary layer
8
9 effect on bacterial attachment. *Biochem Biophys Res Commun* **2015**, *461* (4), 671-
10
11 676.
12
13
14 (25) Wang, J.; et al. Rapid enrichment of denitrifying methanotrophs in a series hollow-
15
16 fiber membrane biofilm reactor. *Sci Total Environ* **2022**, *834*, 155375.
17
18
19 (26) Jones; Susan. Biotechnology: Supercharged: the biofilm anode. *Nature Reviews*
20
21 *Microbiology* **2008**, *6* (3), 173-173.
22
23
24 (27) Baeten, J. E.; et al. Modelling anaerobic, aerobic and partial nitrification-anammox
25
26 granular sludge reactors - A review. *Water Res* **2019**, *149*, 322-341.
27
28
29 (28) Wäsche, S.; et al. Influence of growth conditions on biofilm development and mass
30
31 transfer at the bulk/biofilm interface. *Water Research* **2002**, *36* (19), 4775-4784.
32
33
34 (29) Chen, X.; et al. Model predicted N₂O production from membrane-aerated biofilm
35
36 reactor is greatly affected by biofilm property settings. *Chemosphere* **2021**, *281*,
37
38 130861.
39
40
41
42 (30) Pan, Y.; et al. Substrate Diffusion within Biofilms Significantly Influencing the
43
44 Electron Competition during Denitrification. *Environ Sci Technol* **2019**, *53* (1),
45
46 261-269.
47
48
49 (31) Khlebnikov, A.; et al. Use of a dynamic gassing-out method for activity and
50
51 oxygen diffusion coefficient estimation in biofilms. *Water Science & Technology*
52
53 **1998**, *37* (4-5), 171-175.
54
55
56
57 (32) Chen, X.; et al. A new approach to simultaneous ammonium and dissolved
58
59
60

- methane removal from anaerobic digestion liquor: A model-based investigation of feasibility. *Water Res* **2015**, *85*, 295-303.
- (33) Chen, X.; et al. Achieving complete nitrogen removal by coupling nitrification-anammox and methane-dependent denitrification: A model-based study. *Biotechnol Bioeng* **2016**, *113* (5), 1035-1045.
- (34) Chen, X.; et al. Influences of longitudinal gradients on methane-driven membrane biofilm reactor for complete nitrogen removal: A model-based investigation. *Water Res* **2022**, *220*, 118665.
- (35) Liu, T.; et al. Model-based investigation of membrane biofilm reactors coupling anammox with nitrite/nitrate-dependent anaerobic methane oxidation. *Environ Int* **2020**, *137*, 105501.
- (36) Xie, G. J.; et al. Complete Nitrogen Removal from Synthetic Anaerobic Sludge Digestion Liquor through Integrating Anammox and Denitrifying Anaerobic Methane Oxidation in a Membrane Biofilm Reactor. *Environ Sci Technol* **2017**, *51* (2), 819-827.
- (37) Haynes, W. M. CRC Handbook of Chemistry and Physics. **2014**.
- (38) Martin, K. J.; Nerenberg, R. The membrane biofilm reactor (MBfR) for water and wastewater treatment: principles, applications, and recent developments. *Bioresour Technol* **2012**, *122*, 83-94.
- (39) Reichert, P. AQUASIM 2.0 - Tutorial. Computer program for the identification and simulation of aquatic systems. 1998.
- (40) Nerenberg, R. The membrane-biofilm reactor (MBfR) as a counter-diffusional

- 1
2
3
4 biofilm process. *Curr Opin Biotechnol* **2016**, *38*, 131-136.
5
6
7 (41) Cai, C.; et al. Effect of methane partial pressure on the performance of a membrane
8
9 biofilm reactor coupling methane-dependent denitrification and anammox. *Sci*
10
11 *Total Environ* **2018**, *639*, 278-285.
12
13
14 (42) Zhang, S. F.; et al. Determination of pollutant diffusion coefficients in naturally
15
16 formed biofilms using a single tube extractive membrane bioreactor. *Biotechnology*
17
18 *and Bioengineering* **1998**, *59* (1), 80-89.
19
20
21 (43) Schreyer, H. B.; Coughlin, R. W. Effects of stratification in a fluidized bed
22
23 bioreactor during treatment of metalworking wastewater. *Biotechnology and*
24
25 *Bioengineering* **1999**, *63* (2), 129-140.
26
27
28 (44) Wang, S.; et al. *Biofilm in Moving Bed Biofilm Process for Wastewater Treatment;*
29
30
31
32 Bacterial Biofilms, 2019.
33
34
35 (45) Beer, D. D.; et al. Liquid flow in heterogeneous biofilms. *Biotechnology &*
36
37 *Bioengineering* **2010**, *44* (5), 636-641.
38
39
40 (46) Ni, B.-J.; Yuan, Z. A model-based assessment of nitric oxide and nitrous oxide
41
42 production in membrane-aerated autotrophic nitrogen removal biofilm systems.
43
44 *Journal of Membrane Science* **2013**, *428*, 163-171.
45
46
47 (47) Bishop, P. L.; et al. Effects of biofilm structure, microbial distributions and mass
48
49 transport on biodegradation processes. *Water Science and Technology* **1995**, *31* (1),
50
51
52
53 143-152.
54
55
56
57
58
59
60